Nature. Author manuscript; available in PMC 2014 October 17.

Published in final edited form as:
Nature. 2014 April 17; 508(7496): 416–419. doi:10.1038/nature13037.

Structural basis for translocation by AddAB helicase/nuclease and its arrest at Chi sites

Wojciech W. Krajewski[1,3], **Xin Fu**[1], **Martin Wilkinson**[1], **Nora B. Cronin**[1], **Mark S. Dillingham**[2], and **Dale B. Wigley**[1,*]

[1]Division of Structural Biology, Institute of Cancer Research, Chester Beatty Laboratories, 237 Fulham Road, London SW3 6JB, U.K.

[2]School of Biochemistry, University of Bristol, Medical Sciences Building, University Walk, Bristol BS8 1TD, U.K.

Abstract

In bacterial cells, processing of double-stranded DNA breaks for repair by homologous recombination is dependent upon the recombination hotspot sequence Chi[1,2] and is catalysed by either an AddAB or RecBCD-type helicase-nuclease (reviewed in refs 3, 4). These enzyme complexes unwind and digest the DNA duplex from the broken end until they encounter a Chi sequence[5] whereupon they produce a 3′-single-stranded DNA tail onto which they initiate loading of the RecA protein[6]. Consequently, regulation of the AddAB/RecBCD complex by Chi is a key control point in DNA repair and other processes involving genetic recombination. Here, we report crystal structures of AddAB in complex with different Chi-containing DNA substrates either with or without a nonhydrolysable ATP analogue. Comparison of these structures suggests a mechanism for DNA translocation and unwinding, how the enzyme binds specifically to Chi sequences, and explains how Chi recognition leads to the arrest of AddAB (and RecBCD) translocation that is observed in single molecule experiments[7-9].

We have previously determined the crystal structures of initiation complexes of AddAB and RecBCD bound to a DNA end[10,11]. We have now crystallised AddAB in a translocation-like state by extending the 5′- and 3′-tails of the substrate to mimic an unwound fork (Figure 1 & Extended Data Figure 1). These structures provide additional details of the interaction between the AddA helicase domain and the 3′-tail of the DNA fork (Extended Data Figure 2). The structure of the complex with the non-hydrolysable ATP analogue ADPNP revealed that AddAB contains two ATP-binding sites (Figure 1a). One is located between the helicase domains of AddA, and the other is in the equivalent position between the catalyticallyinactivated helicase domains of AddB. The ATP-binding site in AddA is required for processive DNA translocation and unwinding[12], and is essentially the same as that observed in other SF1 helicases[13]. The ATP-binding site in AddB is important for

---

*To whom correspondence should be addressed: Dale.Wigley@icr.ac.uk.
[3]Present address: CRT Discovery Laboratories, Department of Biological Sciences, Birkbeck, University of London, London, U.K.
Contributions: W.W.K. & D.B.W designed the experiments. W.W.K., X.F., M.W and N.B.C performed the experiments. W.W.K., M.W., M.S.D. and D.B.W. analysed the data and prepared the manuscript.

Accession codes: The coordinates have been deposited at the PDB with accession codes 4CEH, 4CEI and 4CEJ.

stabilising the complex between AddAB and Chi[12]. It contains several residues that are similar to those in AddA, and ADPNP is bound in a similar fashion at both sites (Figure 1b & Extended Data Figure 3). However, there are important differences in residues associated with hydrolysis rather than binding of ATP. For example, essential catalytic glutamate and arginine residues (E408 and R873 in AddA) are replaced in AddB by a glycine and serine, respectively. This suggests that AddB has a much reduced ATPase activity compared to AddA, consistent with biochemical studies[12]. Conservation of an ATP-binding site in AddB further substantiates proposals that the Chi-scanning subunits of RecBCD and AddAB (RecC and AddB, respectively) have evolved from *bona fide* helicase subunits[4,14].

The binding of nucleotide to the AddA subunit induces conformational changes in the motor domains (1A and 2A) comparable to those seen for other SF1 and SF2 helicases[13] (Figure 1a). By contrast, the conformation of the AddB subunit remains unaltered by the binding of ADPNP other than local changes in amino acid side chains. The conformational changes in AddA suggest both a mechanism for ssDNA translocation, similar to that proposed for other SF1 helicases[13,15], and how the complex might unwind DNA (Figure 2). Immediately ahead of the ssDNA motor, the “arm” domain of AddA and the C-terminal nuclease domain of AddB contact the duplex on opposite sides such that they almost encircle the DNA. Upon ATP binding, the 1A and 2A motor domains of AddA move together causing ssDNA to slide by one base across the surface of the 1A domain and the 3′ ssDNA tail to be pulled away from the DNA junction. At the same time, the arm domain pulls the duplex in the opposite direction thereby creating tension that is relieved by unwinding a base pair at the fork junction. When ATP is hydrolysed, the motor domains revert to the open state, domain 1A slides back along the ssDNA towards the junction and the regions of the protein contacting the DNA duplex also slide backwards, to alter the register of DNA contacts by one base pair (see Supplementary Information videos). Hence one cycle of ATP binding and hydrolysis unwinds and translocates the complex by one base pair in common with many other helicases[13]. The unexpected and direct role for the arm domain in this mechanism may provide a molecular basis for the enigmatic secondary translocase activity detected in the structurally related RecBC complex[16].

The AddB subunit is responsible for Chi recognition[10] but the molecular details of this interaction are unknown. To mimic delivery of Chi to the recognition locus, we next prepared a series of DNA substrates that placed a *B.subtilis* Chi sequence (5′-AGCGG[2]) on the 3′-strand at increasing distances from the junction by gradually increasing the length of a “spacer” region (Extended Data Figure 1). These substrates all crystallised with AddAB and ADPNP in the same conditions, space group and unit cell as those lacking Chi. The overall conformation of the protein was the same in all structures, with no electron density attributable to a bound Chi site, with one exception. In the case of the substrate with a seven base spacer, there was strong electron density within the AddB subunit corresponding to a bound Chi sequence (Figure 3) as well as significant alterations in the conformation of the AddA motor domains (discussed below).

Both RecC and AddB have the same fold as a SF1 helicase[10,11] and in AddB even the ATP-binding site is conserved, albeit with changes that likely reduce or abolish ATPase activity (see above). Furthermore, some residues known to affect binding and/or response to Chi in

AddAB and RecBCD are located in positions equivalent to the characteristic helicase motifs[10,17,18]. Consequently, we expected the DNA to bind in a manner similar to that observed for SF1 DNA helicases[13]. The Chi-binding site is indeed located in the same groove as the ssDNA-binding site in SF1 helicases (Figures 3a & 3b). Moreover, residues either side of the Chi sequence interact with the protein principally via the phosphodiester backbone, which is largely similar to ssDNA binding in other DNA helicases which need to bind DNA in a non sequence-specific manner[13]. However, the manner in which the five bases of the Chi sequence interact with the protein is entirely different. Starting with the first residue (adenine), the DNA is flipped by 180° such that the bases point towards, rather than away from, the protein surface. As a result the entire interface with Chi is via the bases, but bounded by the phosphate groups on either side that also make important contacts (see below). This mode of binding is thereby optimised for specificity over affinity: any interaction with the backbone would be sequence-independent, increasing affinity for all DNA sequences rather than specificity for Chi. All five bases of the Chi sequence interact with the protein (Figure 3c). Several residues in AddB that either contact the Chi site directly (Q42, T44, R70, F210) or order residues that contact the bases (F68, W73) had been implicated previously in the recognition or response to Chi[10]. However, this structure reveals a role for several additional residues including some, surprisingly, that are in the AddA subunit (Figure 3c). Many of these have equivalents in RecB and RecC[17] and likely reflects a commonality in the mechanism of Chi regulation in AddAB and RecBCD.

The Chi-binding site extends across from the AddB subunit into the AddA nuclease domain which has the same fold as λ-exonuclease[19]. The structure of λ-exonuclease complexed with DNA[20] identified the importance of the 5′-phosphate of the substrate for both binding and catalysis. The function of an arginine residue (R28) that plays a key role in this contact is replaced by a tyrosine (Y1204) in AddA (Figure 3d). However, in λ-exonuclease, additional contacts with this phosphate moiety involve residues T33-S35, a region that is conserved in the nuclease domain of AddA (S1015-S1017) within the linker connecting the helicase and nuclease domains. These residues coordinate the equivalent position in the phosphodiester backbone on the 3′ side of the final G of the Chi sequence. A similar motif is conserved in the AddB nuclease domain and likely contributes in an equivalent manner to binding of the 5′-tail. As the 3′ ssDNA tail continues beyond the Chi sequence and enters the AddA nuclease domain, the conformation flips back by 180° so that the principal contacts are once again with the phosphodiester backbone rather than the bases.

Single-molecule experiments with RecBCD[7,8] and AddAB[9] revealed that both complexes show interesting behaviour when encountering a Chi sequence. In each case, the complexes are unwinding DNA at several hundred base pairs per second before suddenly pausing at Chi for several seconds. After this pause, the complexes resume translocation but usually at a lower speed and with modified properties such that the complex is no longer able to recognise a second Chi site suggesting that the enzyme remains associated with the original Chi site thereby blocking binding in a subsequent encounter. Initially, two explanations for the pause were proposed for RecBCD[7]. The first was that because the RecB and RecD motors run at different speeds[21] and the RecD motor becomes inactivated at Chi[22], (although remains associated with the complex[23,24]), the pause at Chi was a consequence of the slower (RecB) motor “catching up” with additional bases unwound by the faster RecD

before net translocation by RecB could recommence. The change in translocation speed observed for RecBCD was attributed to a change in the nature of the lead motor from the faster RecD before Chi to the slower RecB after Chi. However, subsequent work showed that a mutant RecBCD enzyme with an inactivated RecD subunit displays the same pausing behaviour[8], as does the single-motor AddAB complex[9], ruling this out as an explanation.

The second proposal was that a Chi-dependent conformational change takes place during the pause that is required before translocation can recommence[7,23]. During the pause, the enzyme is stalled in an altered, but unknown, conformational state until it reactivates to a form that can recommence translocation. However, no information about this Chi-dependent stalled conformation could be obtained from the single-molecule experiments.

Our structure of the Chi-bound state of AddAB now reveals the nature of the conformational change that takes place upon encountering Chi. Unexpectedly, the 1A and 2A motor domains of the AddA subunit adopt the conformation for the complex without bound nucleotide despite being grown under the same conditions as the ADPNP complex and crystallising in the same space group and unit cell. Importantly, the ATP-binding sites of AddA and AddB are both occupied with a bound ADPNP (Extended Data Figure 3). Consequently, when Chi is bound to the AddB subunit, the AddA motor domains are unable to adopt the usual nucleotide bound closed conformation thereby blocking DNA translocation and explaining the pause seen in single-molecule experiments[7-9]. We have now determined several structures of Chi-bound complexes from different crystals and these show that although domain 1A is consistently in an orientation similar to that in the binary complex, the 2A domain adopts a range of non-canonical conformations (Extended Data Figure 4) suggesting domain 1A is locked but domain 2A becomes uncoupled and is able to adopt multiple states. Hence, the paused Chi-bound state may well remain able to hydrolyse ATP without translocating, rather like a motor idling without the gearbox engaged, until a subsequent conformational change allows the complex to re-engage and recommence translocation.

Although our structure reveals how the pause is initiated, the reason for the pause remains a point for speculation. One possibility is that the protein requires a slow conformation change to take place before the complex is proficient for the next phase of the reaction, namely the loading of RecA protein. Data for both RecBCD and AddAB suggest this may involve the opening of a protein gateway to allow extrusion of a ssDNA loop[10,17,25]. Interestingly, the structure reveals a direct link from the Chi-binding site (R132) to one of the residues (E129) that forms part of a proposed latch (Figure 3e) responsible for the opening of this exit channel, although the latch remains in the closed conformation in this structure. It might also be that the final DNA cleavage event on the Chi-containing strand has to take place before translocation resumes and RecA begins to load. This would act as a failsafe mechanism to ensure the production of an appropriate substrate for extension by the action of DNA polymerase following RecA-dependent strand invasion. Consistent with this view, a nuclease-defective RecBCD complex is not able to load RecA protein at Chi[26]. The work we present here captures several intermediates on the AddAB repair pathway (Extended Data Figure 5) but further work is required to understand how the complex is reactivated

following the stall at Chi, thereby resuming DNA unwinding and the loading of RecA protein to initiate homologous recombination.

Methods

Cloning, protein expression and purification

The nuclease-dead AddAB mutant (pCOLADuet-1-AddA^{D1172A}B^{D961A}) described previously[27] was modified to include a TEV protease cleavable His_6-tag at the N-terminus of the AddA subunit. B834 (DE3) cells harbouring the AddAB plasmid were grown at 37°C in LB medium containing 50 μg/ml kanamycin to an OD of 0.4, induced with 1 mM IPTG and grown at 27°C for 3h. Cells were harvested and frozen at -80°C until further use. For protein purification, thawed cells were resuspended and lysed in the lysis buffer (50 mM Tris-HCl pH 7.5, 150 mM NaCl, 1 mM DTT, 2 SigmaFast Protease inhibitor cocktail tablets, 0.03 mg/ml DNase I, a pinch of lysozyme) using EmulsiFlex homogeniser (Avestin). After centrifugation, polyethylenimine and ammonium sulfate (AS) precipitations were carried out essentially as described previously[27], except that for the latter AS was added to a final concentrations of 60%. AS pellets were dissolved in the HisTrap binding buffer (50 mM Tris-HCl pH 8.0, 300 mM NaCl, 20 mM imidazole, 1 mM DTT) and filtered through a 0.45-μm syringe filter. The protein was loaded onto a HisTrap FF column (GE Healthcare) and washed with HisTrap binding buffer. To remove DNA from AddAB, the bound protein was washed with a high-salt (20 mM Tris-HCl pH 8.0, 1 M NaCl, 20 mM imidazole, 1 mM DTT) and low-salt (20 mM Tris-HCl pH 8.0, 100 mM NaCl, 20 mM imidazole, 1 mM DTT) wash buffers. AddAB was eluted from the column with the elution buffer (20 mM Tris-HCl pH 8.0, 100 mM NaCl, 250 mM imidazole, 1 mM DTT). The pooled peak fractions containing AddAB were diluted with 20 mM Tris-HCl pH 8.0, 1 mM DTT to a conductivity of 7 mS/cm before loading onto the HiTrap heparin column (GE Healthcare). AddAB was eluted with a linear gradient from 50 mM to 500 mM NaCl over 30 column volumes. To pooled AddAB fractions, TEV protease was added at 1:20 w/w ratio, and the solution was dialysed against the dialysis buffer (20 mM Tris-HCl pH 7.5, 100 mM NaCl, 1 mM DTT) overnight at 4°C. To remove the His_6-tag and any uncleaved protein, the dialysate was passed through a HisTrap FF column. The flow-through was collected and loaded onto a MonoQ column (GE Healthcare). The protein was eluted with a linear gradient from 200 mM to 600 mM NaCl over 30 column volumes. The pooled peak fractions containing AddAB were diluted with 20 mM Tris-HCl pH 7.5, 1 mM DTT to a conductivity of 10 mS/cm and concentrated to 10 mg/ml using a Vivaspin concentrator (GE Healthcare). The protein was aliquoted, flash-frozen in liquid nitrogen and stored at -80°C.

Crystallization

The DNA substrates used for crystallization were prepared as described previously[11]. Crystals of AddAB complexes were obtained by vapour diffusion in hanging drops at 12°C. For the AddAB/023/ADPNP structure, protein was incubated with the DNA substrate : (5′-TTTTTTTCTAATGCGAGCACTGCTATTCCCTAGCAGTGCTCGCATTAGATTTTGTTTTTTAGCGG-3′) at 1:1.3 molar ratio for 30 min on ice. The AddAB/DNA complex was then purified by gel filtration on a Superdex 200 column (GE Healthcare) and concentrated to 5.5 mg/ml for crystallization. ADPNP and magnesium chloride were added to the

complex to a final concentration of 2 and 5 mM, respectively. Crystals were obtained by mixing equal volumes of protein and mother liquor consisting of 17.5% polyethylene glycol 1500, 0.1M Hepes pH 7.5, 0.25 M NaCl, 0.1 M sodium formate, 0.1 M magnesium chloride. Crystals were cryoprotected by the addition of the reservoir solution supplemented with 30% ethylene glycol, and flash-frozen in liquid nitrogen.

For the AddAB/023 structure, protein was mixed with the DNA substrate (as above) at 1:1.3 molar ratio and incubated for 30 min on ice prior to crystallization. Crystals were obtained by mixing two volumes of protein and one volume of mother liquor consisting of 15% polyethylene glycol 4000, 0.1M Tris-HCl pH 7.5, 0.8 M sodium formate. To improve crystal quality, microseeding was used. Crystals were cryoprotected and flash frozen as described above.

For the AddAB/027/ADPNP structure, protein was mixed with the DNA substrate (5′-TTTTTTTCTAATGCGAGCACTGCTATTCCCTAGCAGTGCTCGCATTAGATTTTGTTTTTTTAGCGGTTTT-3′) at 1:1.3 molar ratio in the presence of 2 mM ADPNP and 5 mM magnesium chloride. The complex was incubated for 30 min on ice prior to crystallization. Crystals were obtained by mixing two volumes of protein and one volume of mother liquor consisting of 11% polyethylene glycol 4000, 0.1M Tris-HCl pH 7.5, 0.1 M magnesium acetate. Microseeding was used to improve crystal quality. Crystals were cryoprotected and flash frozen as described above.

Structure determination and refinement

For the AddAB/023/ADPNP structure, a 2.8-Å diffraction data set was collected at the Diamond Light Source (DLS) beamline IO4 at a wavelength of 0.98Å and a temperature of 100K. The data were integrated and scaled using XDS and XSCALE[28]. Intensities were converted to structure factors using CTRUNCATE[29].The crystals belonged to space group $P2_1$ with one AddAB/DNA complex in the asymmetric unit. The structure was determined by molecular replacement (MR) in PHASER[30] using AddAB/DNA complex (PDB ID: 3U4Q) as a search model. To account for conformational changes, the model was first subjected to rigid-body refinement of the individual AddA and AddB subdomains. Alternating rounds of model building and refinement were carried using COOT[31] and PHENIX[32] respectively. The final model had good geometry with 0.1% of residues outside the allowed regions.

For the AddAB/023 structure, a 3.2-Å diffraction data set was collected at the DLS beamline IO2 at a wavelength of 0.98Å and a temperature of 100K. The data were processed as described above. The crystals belonged to space group P1 with one AddAB/DNA complex in the unit cell. The structure was determined by MR in PHASER using AddAB/023/ADPNP structure as a search model. Model building and refinement were carried out as described above. The final model had good geometry with 0.1% of residues outside the allowed regions.

For the AddAB/027/ADPNP structure, a 3.0Å diffraction data set was collected at the DLS beamline I24 at a wavelength of 0.969Å and a temperature of 100K. The crystals belonged to space group $P2_1$ with one AddAB/DNA complex in the asymmetric unit. The structure

was determined by MR in PHASER using the AddAB/023/ADPNP structure as a search model. Model building and refinement were carried out as described above. The structures were validated using MOLPROBITY[33] as implemented in PHENIX. The final model had good geometry with 0.2% of residues outside the allowed regions.

Supplementary Material

Refer to Web version on PubMed Central for supplementary material.

Acknowledgments

We thank the ESRF and Diamond synchrotrons for access to beamlines. The work was funded by the Royal Society, the Wellcome Trust and the European Research Council (MSD), Cancer Research UK (DBW) and EMBO (WWK).

References

1). Lam ST, Stahl MM, McMilin KD, Stahl FW. Rec-mediated recombinational hot spot activity in bacteriophage lambda. II. A mutation which causes hot spot activity. Genetics. 1974; 77:425–33. [PubMed: 4415485]

2). Chédin F, Noirot P, Biaudet V, Ehrlich SD. A five-nucleotide sequence protects DNA from exonucleolytic degradation by AddAB, the RecBCD analogue of Bacillus subtilis. Mol. Microbiol. 1998; 29:1369–77. [PubMed: 9781875]

3). Dillingham MS, Kowalczykowski SC. RecBCD enzyme and the repair of double-stranded DNA breaks. Microbiol Mol Biol Rev. 2008; 72:642–671. [PubMed: 19052323]

4). Wigley DB. Bacterial DNA repair: recent insights into the mechanism of RecBCD, AddAB and AdnAB. Nat. Rev. Microbiol. 2013; 11:9–13. [PubMed: 23202527]

5). Ponticelli AS, Schultz DW, Taylor AF, Smith GR. Chi-dependent DNA strand cleavage by RecBC enzyme. Cell. 1985; 41:145–51. [PubMed: 3888404]

6). Anderson DG, Kowalczykowski SC. The translocating RecBCD enzyme stimulates recombination by directing RecA protein onto ssDNA in a chi-regulated manner. Cell. 1997; 90:77–86. [PubMed: 9230304]

7). Spies M, Bianco PR, Dillingham MS, Handa N, Baskin RJ, Kowalczykowski SC. A molecular throttle: the recombination hotspot chi controls DNA translocation by the RecBCD helicase. Cell. 2003; 114:647–54. [PubMed: 13678587]

8). Spies M, Amitani I, Baskin RJ, Kowalczykowski SC. RecBCD enzyme switches lead motor subunits in response to chi recognition. Cell. 2007; 131:694–705. [PubMed: 18022364]

9). Carrasco C, Gilhooly NS, Dillingham MS, Moreno-Herrero F. On the mechanism of recombination hotspot scanning during double-stranded DNA break resection. Proc Natl Acad Sci U S A. 2013; 110:E2562–71. [PubMed: 23798400]

10). Saikrishnan K, Yeeles JT, Gilhooly NS, Krajewski WW, Dillingham MS, Wigley DB. Insights into Chi recognition from the structure of an AddAB-type helicase-nuclease complex. EMBO J. 2012; 31:1568–78. [PubMed: 22307084]

11). Singleton MR, Dillingham MS, Gaudier M, Kowalczykowski SC, Wigley DB. Crystal structure of RecBCD enzyme reveals a machine for processing DNA breaks. Nature. 2004; 432:187–193. [PubMed: 15538360]

12). Yeeles JT, Gwynn EJ, Webb MR, Dillingham MS. The AddAB helicase-nuclease catalyses rapid and processive DNA unwinding using a single Superfamily 1A motor domain. Nucleic Acids Res. 2011; 39:2271–85. [PubMed: 21071401]

13). Singleton MR, Dillingham MS, Wigley DB. Structure and mechanism of helicases and nucleic acid translocases. Annu Rev Biochem. 2007; 76:23–50. [PubMed: 17506634]

14). Unciuleac MC, Shuman S. Characterization of the mycobacterial AdnAB DNA motor provides insights into the evolution of bacterial motor-nuclease machines. J. Biol. Chem. 2010; 285:2632–2641. [PubMed: 19920138]

15). Velankar SS, Soultanas P, Dillingham MS, Subramanya HS, Wigley DB. Crystal structures of complexes of PcrA DNA helicase with a DNA substrate indicate an inchworm mechanism. Cell. 1999; 97:75–84. [PubMed: 10199404]

16). Wu CG, Bradford C, Lohman TM. Escherichia coli RecBC helicase has two translocase activities controlled by a single ATPase motor. Nat. Struct. Mol. Biol. 2010; 17:1210–7. [PubMed: 20852646]

17). Handa N, Yang L, Dillingham MS, Kobayashi I, Wigley DB, Kowalczykowski SC. Molecular determinants responsible for recognition of the single-stranded DNA regulatory sequence, χ, by RecBCD enzyme. Proc. Natl. Acad. Sci. U.S.A. 2012; 109:8901–8906. [PubMed: 22603794]

18). Yang L, Handa N, Liu B, Dillingham MS, Wigley DB, Kowalczykowski SC. Mutation of χ-recognition by RecBCD reveals a regulated molecular latch and suggests a channel-bypass mechanism for biological control. Proc. Natl. Acad. Sci. U.S.A. 2012; 109:8907–8912. [PubMed: 22603793]

19). Kovall R, Matthews BW. Toroidal structure of lambda-exonuclease. Science. 1997; 277:1824–7. [PubMed: 9295273]

20). Zhang J, McCabe KA, Bell CE. Crystal structures of lambda exonuclease in complex with DNA suggest an electrostatic ratchet mechanism for processivity. Proc. Natl. Acad. Sci. U.S.A. 2011; 108:11872–7. [PubMed: 21730170]

21). Taylor AF, Smith GR. RecBCD enzyme is a DNA helicase with fast and slow motors of opposite polarity. Nature. 2003; 423:889–893. [PubMed: 12815437]

22). Thaler DS, Sampson E, Siddiqi I, Rosenberg SM, Thomason LC, Stahl FW, Stahl MM. Recombination of bacteriophage lambda in recD mutants of Escherichia coli. Genome. 1989; 31:53–67. [PubMed: 2556327]

23). Dohoney KM, Gelles J. Chi-sequence recognition and DNA translocation by single RecBCD helicase/nuclease molecules. Nature. 2001; 409:370–4. [PubMed: 11201749]

24). Handa N, Bianco PR, Baskin RJ, Kowalczykowski SC. Direct visualization of RecBCD movement reveals cotranslocation of the RecD motor after chi recognition. Mol. Cell. 2005; 17:745–50. [PubMed: 15749023]

25). Wong CJ, Rice RL, Baker NA, Ju T, Lohman TM. Probing 3′-ssDNA loop formation in E. coli RecBCD/RecBC-DNA complexes using non-natural DNA: a model for “Chi” recognition complexes. J. Mol. Biol. 2006; 362:26–43. [PubMed: 16901504]

26). Anderson DG, Churchill JJ, Kowalczykowski SC. A single mutation, RecB(D1080A) eliminates RecA protein loading but not Chi recognition by RecBCD enzyme. J. Biol. Chem. 1999; 274:27139–44. [PubMed: 10480929]

Extended Data References

27). Yeeles JT, Cammack R, Dillingham MS. An iron-sulfur cluster is essential for the binding of broken DNA by AddAB-type helicase-nucleases. J Biol Chem. 2009; 284:7746–7755. [PubMed: 19129187]

28). Kabsch W. XDS. Acta Crystallogr D Biol Crystallogr. 2010; 66:125–132. [PubMed: 20124692]

29). Collaborative Computational Project, Number 4. The CCP4 suite: programs for protein crystallography. Acta Crystallogr D Biol Crystallogr. 1994; 50(Part 5):760–763. [PubMed: 15299374]

30). McCoy AJ, Grosse-Kunstleve RW, Adams PD, Winn MD, Storoni LC, Read RJ. Phaser crystallographic software. J Appl Cryst. 2007; 40:658–674. [PubMed: 19461840]

31). Emsley P, Lohkamp B, Scott WG, Cowtan K. Features and development of Coot. Acta Crystallogr D Biol Crystallogr. 2010; 66:486–501. [PubMed: 20383002]

32). Adams PD, Afonine PV, Bunkoczi G, Chen VB, Davis IW, Echols N, Headd JJ, Hung LW, Kapral GJ, Grosse-Kunstleve RW, McCoy AJ, Moriarty NW, Oeffner R, Read RJ, Richardson DC, Richardson JS, Terwilliger TC, Zwart PH. PHENIX: a comprehensive Python-based system

for macromolecular structure solution. Acta Crystallogr D Biol Crystallogr. 2010; 66:213–221. [PubMed: 20124702]

33). Davis IW, Leaver-Fay A, Chen VB, Block JN, Kapral GJ, Wang X, Murray LW, Arendall WB III, Snoeyink J, Richardson JS, Richardson DC. MolProbity: all-atom contacts and structure validation for proteins and nucleic acids. Nucleic Acids Res. 2007; 35:W375–W383. [PubMed: 17452350]

Europe PMC Funders Author Manuscripts

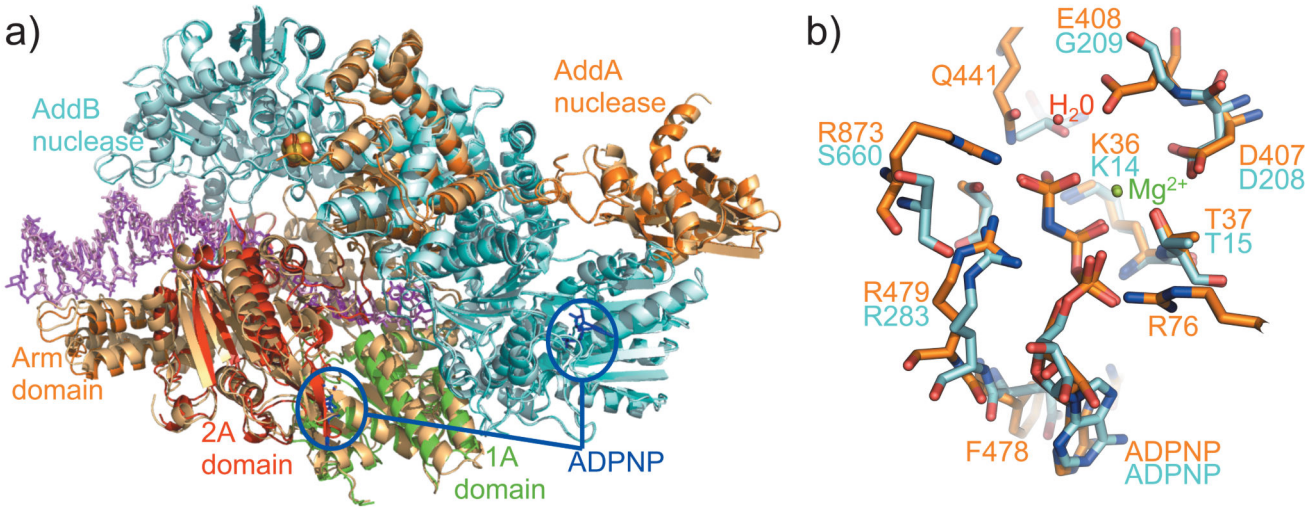

Figure 1. Structure of the binary and ternary complexes.

a) Comparison of the binary and ternary (ADPNP) complexes. AddA is shown in beige (binary) and orange (ADPNP) but with the motor domains of AddA in the ADPNP complex in green and red, AddB in light cyan (binary) and cyan (ADPNP), the DNA is shown in pink (binary) and purple (ADPNP), bound ADPNP molecules in blue sticks, and the iron-sulphur cluster as spheres. b) Overlay of ATP-binding sites in AddA (orange) and AddB (cyan). Although a bound magnesium ion is superimposable in both sites, a bound water molecule, positioned for attack of the γ-phosphate, is only evident in the AddA site.

Europe PMC Funders Author Manuscripts

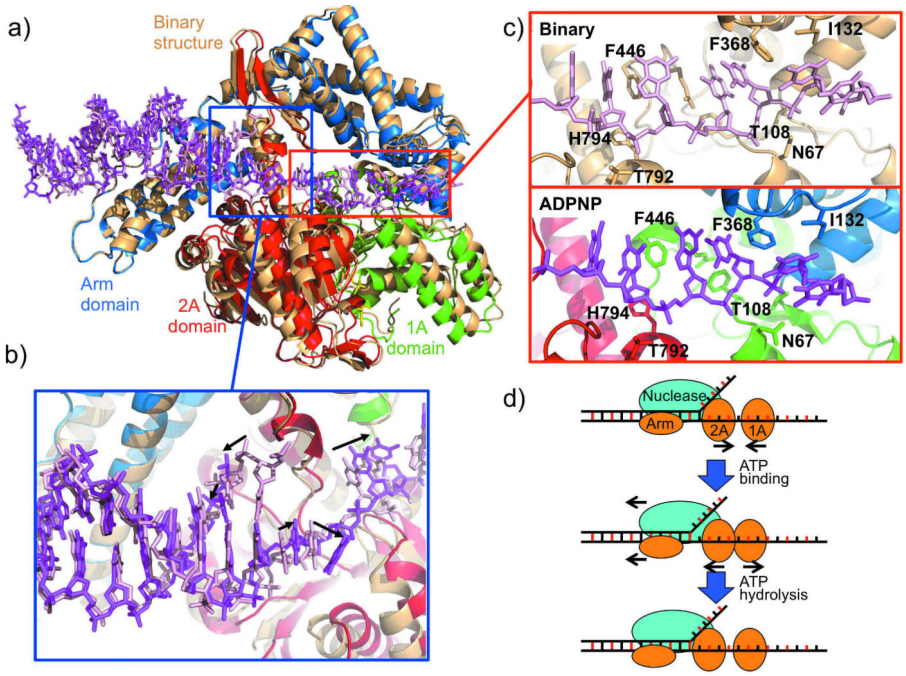

Figure 2. Proposed mechanism of unwinding and translocation.

a) Superposition of the structures on the arm domain illustrates the stretching of the DNA junction that occurs when ATP-binding induces movement of the 1A and 2A domains. For clarity only the DNA and domains 1A, 1B and 2A are shown. The binary complex is coloured in beige (protein) and pink (DNA) while the ADPNP structure is coloured as labelled in the figure with the DNA in purple. b) The register of contacts between (i) the arm domain and DNA duplex and, (ii) the 2A domain and ssDNA remains the same but their separation increases upon ATP binding. The strain in the duplex is relieved by unwinding of the duplex causing disruption of a single base pair at the junction. Arrows highlight some of the important movements of the DNA. c) Contacts with the ssDNA tail change register by a single base upon ATP binding as the DNA slides across the surface of domain 1A. d) Cartoon summarising the minimal steps in the unwinding mechanism. Upon ATP binding, the 1A and 2A domains of AddA close and the conformational change slides along the 3′-ssDNA tail across the surface of the 1A domain by one base. At the same time, the spacing between the arm domain and the 2A domain increases introducing stress into the duplex causing it to unwind a base pair at the junction. After hydrolysis of ATP, the 1A and 2A domains relax to the open conformation causing the 2A domain to slide across the ssDNA. At the same time, the arm domain and the nuclease domain of AddB slide by one base pair along the duplex. This simple two-step process identifies a minimal set of conformational changes that are required to unwind the DNA but does not preclude other intermediates.

Europe PMC Funders Author Manuscripts

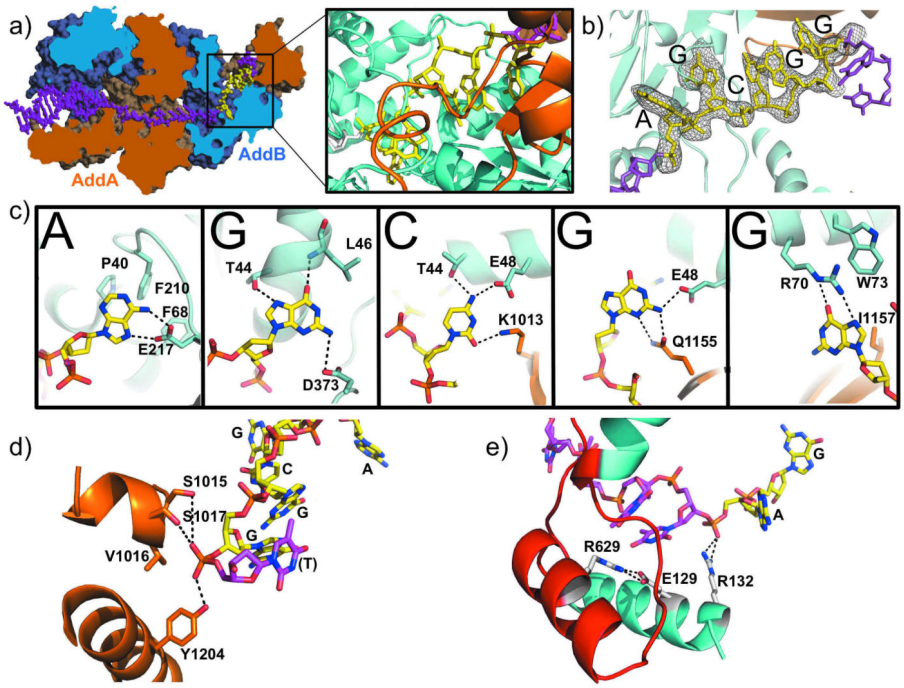

Figure 3. The complex of AddAB bound to Chi.

a) Cutaway space filling representation of the ADPNP/Chi complex showing the long channel through the complex, along which the DNA runs. DNA is purple but with the Chi residues in yellow (inset shows close up of the Chi site but in ribbon format), b) difference electron density, (Fo-Fc, contoured at 2.5σ corresponding to the five residues of the Chi site, with the final structure overlaid for reference, c) details of interactions with each base of the Chi sequence, d) binding site for the phosphate group at the 3′-end of the Chi sequence (carbon atoms yellow), e) link between the phosphate binding site at the 5′-end of the Chi residues (yellow) and the latch residues (red).

Europe PMC Funders Author Manuscripts